

Supplementary Material

Metal Oxide Double Layer Capacitors by Electrophoretic Deposition of Metal Oxides. Fabrication, Electrical Characterization and Defect Analysis Using Positron Annihilation Spectroscopy

Rudolf C. Hoffmann¹, Nico Koslowski¹, Shawn Sanctis¹, Maciej O. Liedke², Andreas Wagner², Maik Butterling², and Jörg J. Schneider^{1*}

Description of analytical instruments:

Atomic Force Microscopy (AFM): CP-II (Bruker-Veeco), tapping mode, 1 Hz, silicon cantilevers (T 3.75 μm , L 125 μm , W 35 μm , f_0 300 kHz, k 40 N/m).

Thermogravimetry (TG): TG209F1-Iris (Netzsch). Samples were measured in oxygen or argon at a heating rate of 10 $^{\circ}\text{C}/\text{min}$ in the range of 30 - 600 $^{\circ}\text{C}$ in aluminium crucibles.

IR spectroscopy (IR): Nicolet iS10 (Thermo Scientific) with TG/IR interface.

Dynamic Light Scattering (DLS): Zetasizer Nano (Malvern). Samples were measured in 10 mm quartz cuvettes. Viscosities and refractive indices for methoxyethanol/acetonitrile mixtures were taken from M.I. Aralaguppi, C.V. Jadar, T.M. Aminabhavi, *J. Chem. Eng. Data* **1996**, *41*, 1307-1310.

X-Ray diffraction (XRD): Miniflex 600 (Rigaku), Cu-K α radiation, 600 W in Bragg-Brentano geometry.

SEM: XL30FEG (Philips) operated at 20 kV. Samples were grounded with a small amount of silver paste at the edges. No further coating with metal (e.g. by sputtering) was applied.

Ellipsometry: M-2000 (J.A. Woollam). Data were obtained using a diode-array rotating compensator and a xenon light source over a wavelength range of 245–900 nm. Samples investigated in this work were modelled using J.A. Woollam Co. WVase32 software. Refractive indices for ITO and glass were obtained by measuring an uncoated ITO/glass substrate. Optical constants of ZnO films were fitted in addition to the thickness of ZnO layer using an effective medium approximation to account for porosity (Fig. S16). The known thickness of ITO was kept constant in all evaluation procedures.

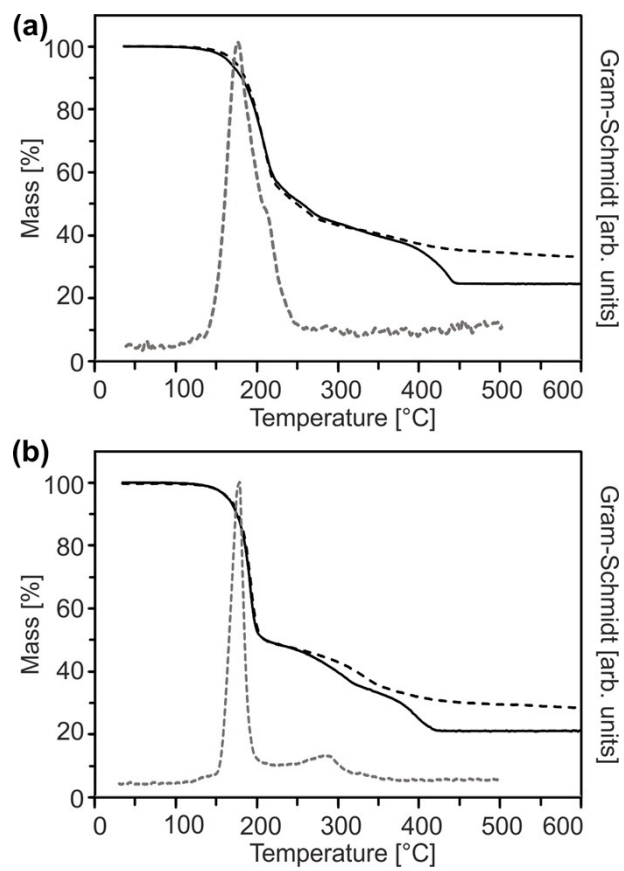


Fig S1: Thermogravimetric mass loss curve in air (solid black) and argon (dashed black) as well as corresponding Gram-Schmidt signal (dashed grey) of (a) (3) and (b) (4).

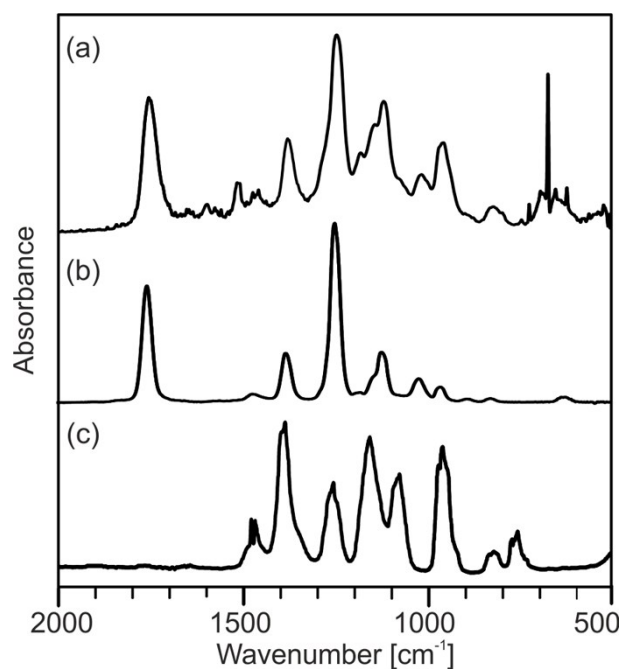


Fig S2: Gas phase IR spectra corresponding to (a) the maximum of the Gram-Schmidt signal in Figure S1 from the decomposition of precursor (**2**) as well as reference spectra of (b) iso-propylacetate and (b) iso-propanol.

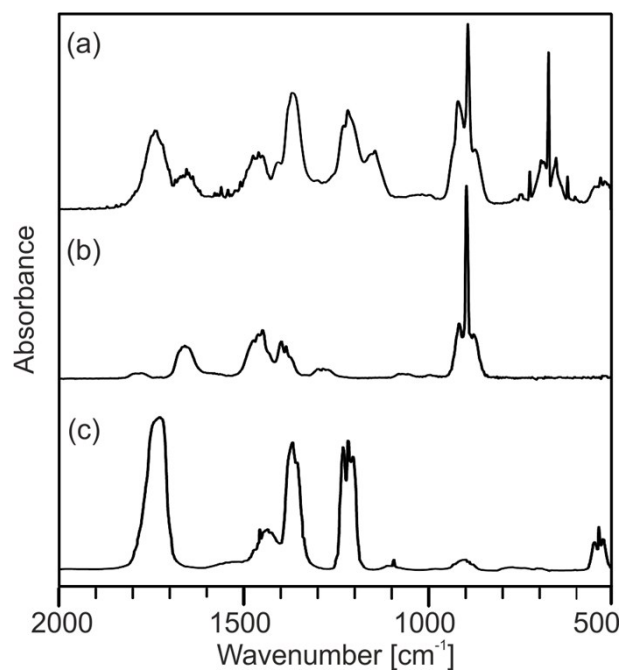


Fig S3: Gas phase IR spectra corresponding to (a) the maximum of the Gram-Schmidt signal in Figure S1 from the decomposition of precursor (**4**) as well as reference spectra of (b) iso-butene and (b) acetone.

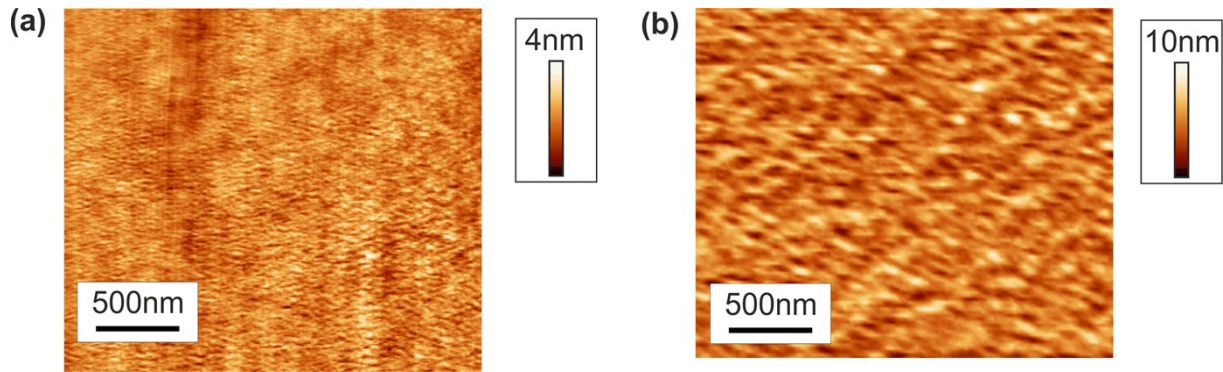


Fig S4: AFM topography of PMMA films (thickness ~ 350 nm in both cases) by spincoating from anisole/acetonitrile (v:v; 90:10) after annealing in argon (a) at 60 °C (RMS 0.3 nm) and (b) at 90 °C (RMS 1.4 nm).

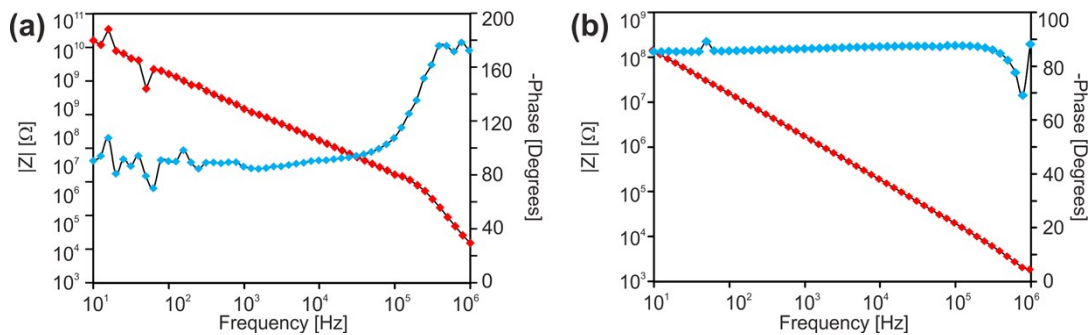


Fig S5: Bode-plots for PMMA films (thickness ~ 300 nm in both cases) by spincoating from anisole after annealing in argon at (a) 60 °C and (b) 90 °C. Gold electrodes had 1000 μm diameter. Dielectric constant and loss can be determined from (b) as κ 3.05 ± 0.11 ; θ 2.07° at 10^5 Hz.

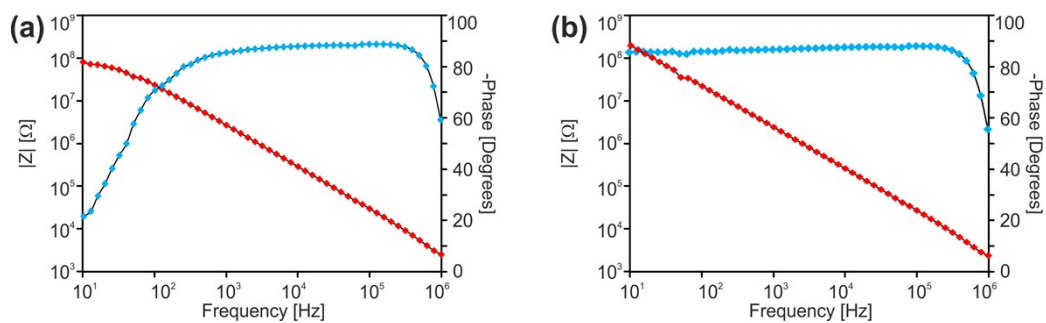


Fig S6: Bode-plots for PMMA films (thickness ~ 350 nm in both cases) by spincoating from anisole/acetonitrile (v:v; 90:10) after annealing in argon at (a) 60 °C and (b) 90 °C. Gold electrodes had 1000 μm diameter. Dielectric constant and loss can be determined from (b) κ 2.97 ± 0.09 ; θ 1.97° at 10^5 Hz

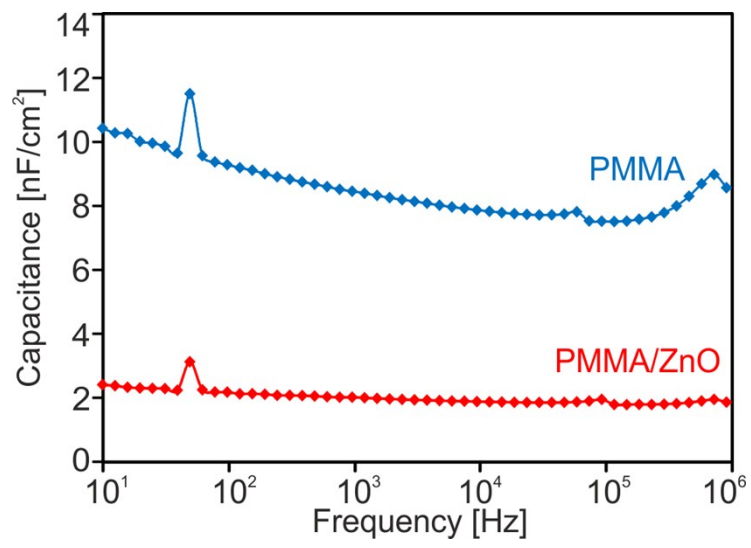


Fig S7: Capacitance of MOS diode (ZnO 60 nm, PMMA 300 nm, red colour) in comparison to control capacitor (PMMA 300 nm, blue colour).

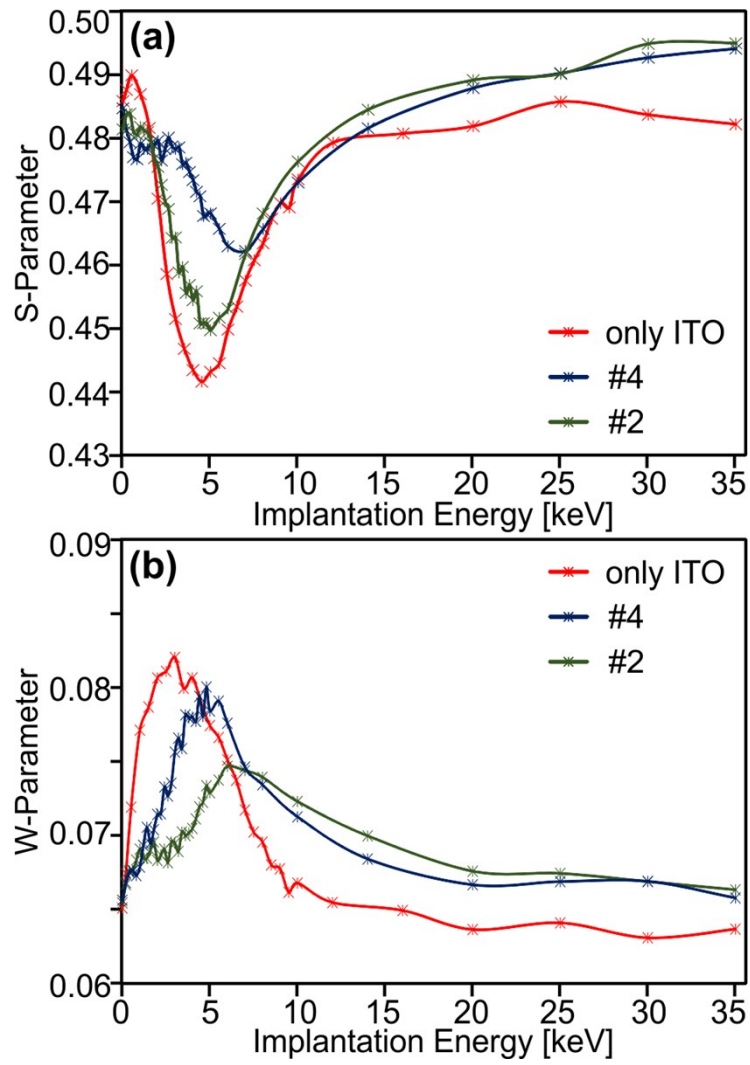


Fig S8: (a) S and (b) W parameter as function of implantation energy for ZnO coated substrates (samples #2 and #4) as well as for an uncoated ITO/glass electrodes.

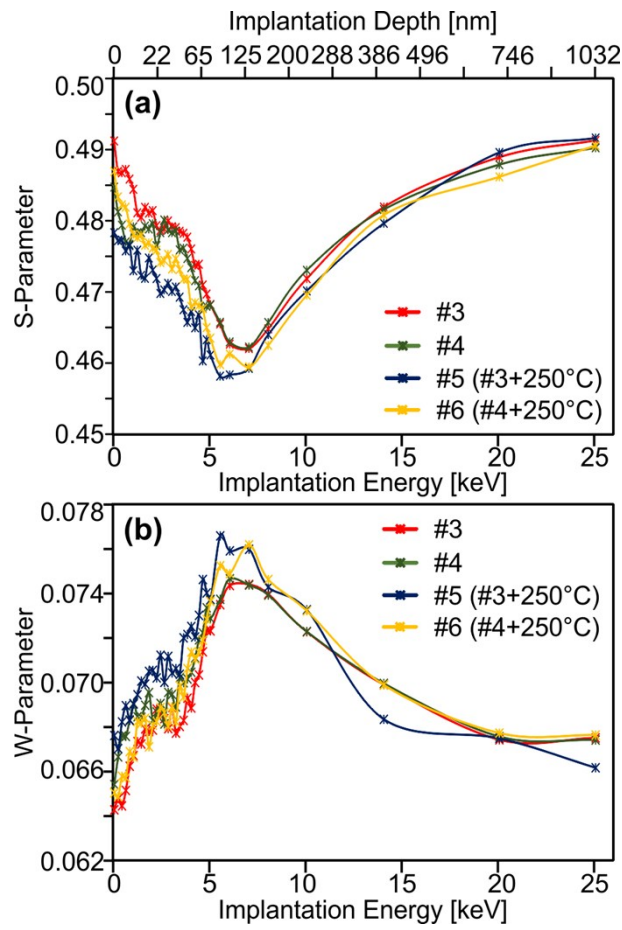


Fig S9: (a) S and (b) W parameter as function of implantation energy as well as corresponding calculated values for implantation depth in ZnO. Comparison of as-deposited and annealed samples.

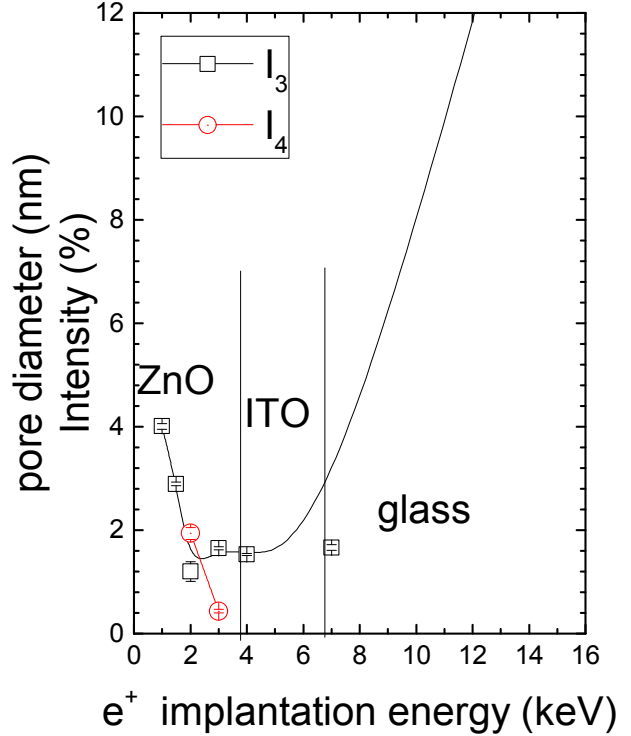
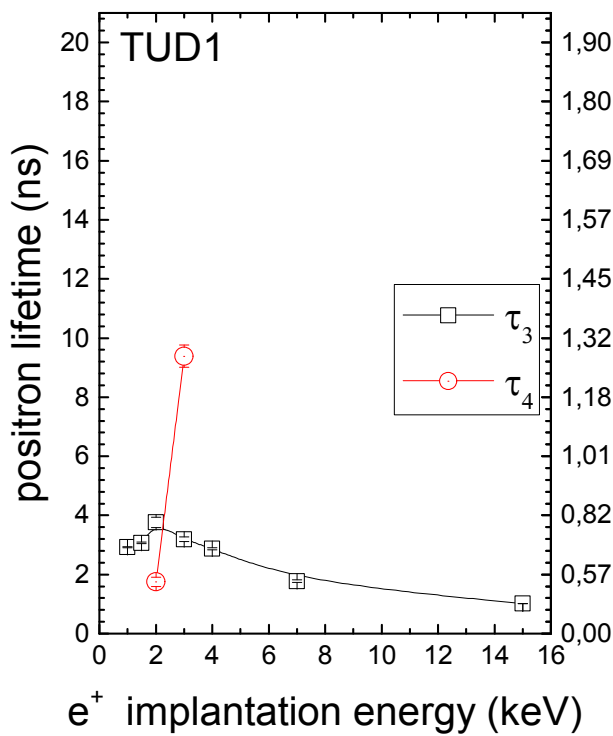
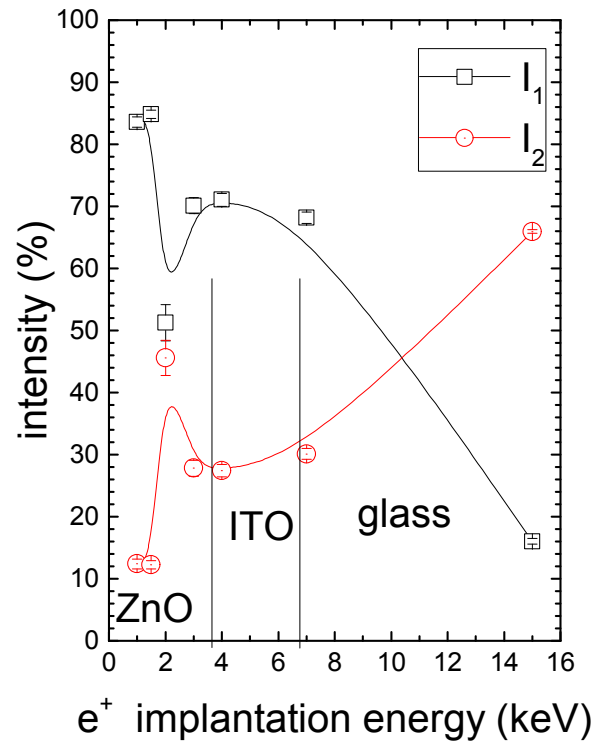
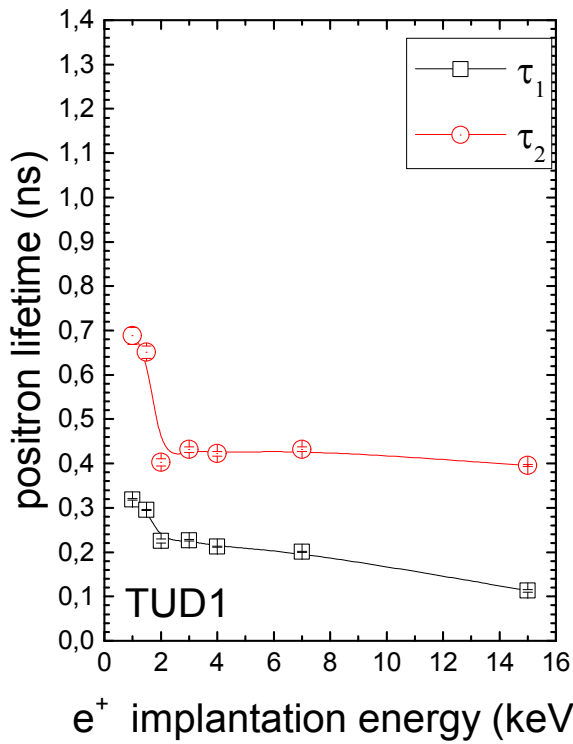


Fig S10: Depth profile derived from the curve fitting of the PALS spectra of ZnO film on ITO/glass substrate (*sample 1*) depicting values of the lifetime component τ_1 - τ_4 in dependence of positron implantation energy. (a) Lifetime components τ_1 and τ_2 . (b) Lifetime components τ_3 and τ_4 as well pore diameters calculated therefrom.

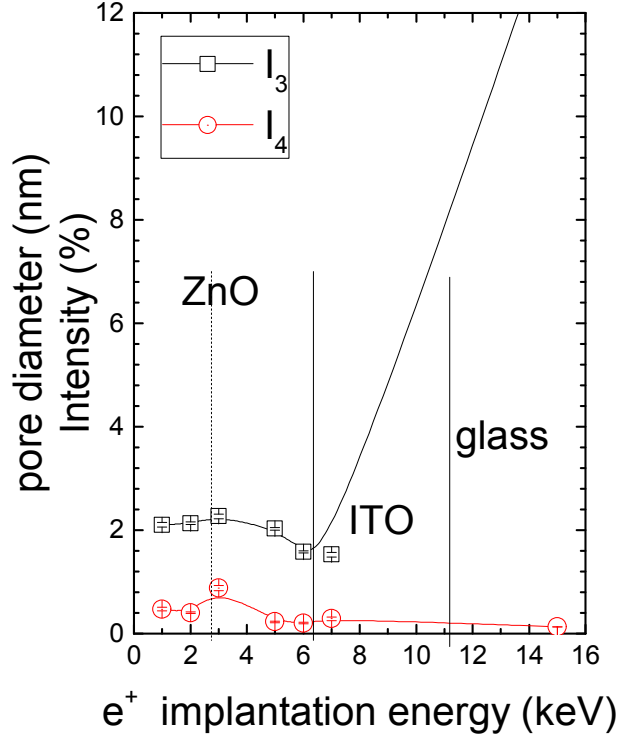
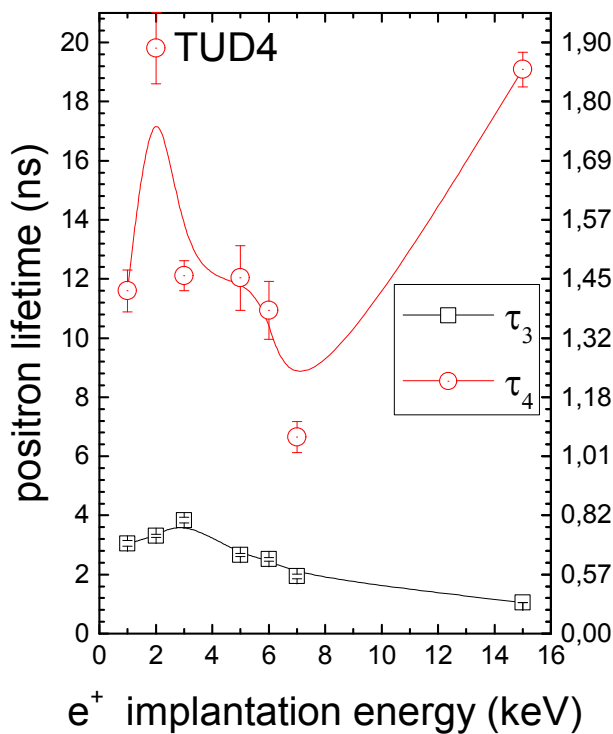
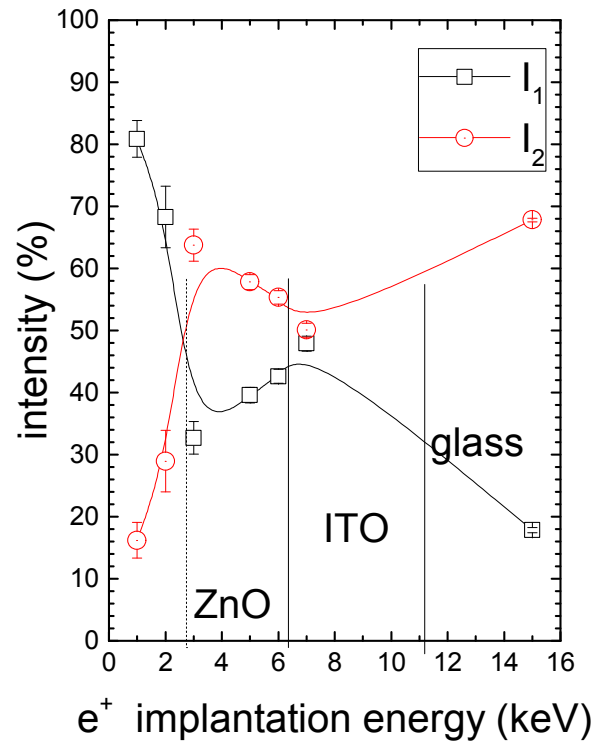
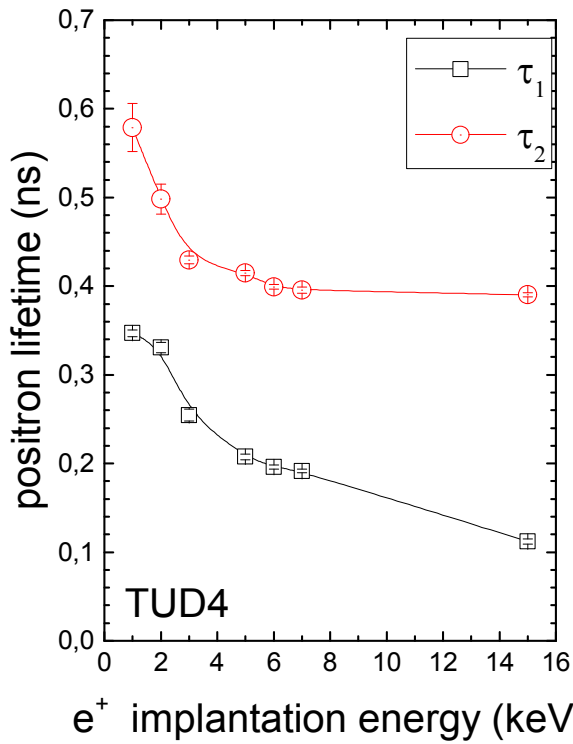


Fig S11: Depth profile derived from the curve fitting of the PALS spectra of ZnO film on ITO/glass substrate (*sample 2*) depicting values of the lifetime component τ_1 - τ_4 in dependence of positron implantation energy. (a) Lifetime components τ_1 and τ_2 . (b) Lifetime components τ_3 and τ_4 as well pore diameters calculated therefrom.

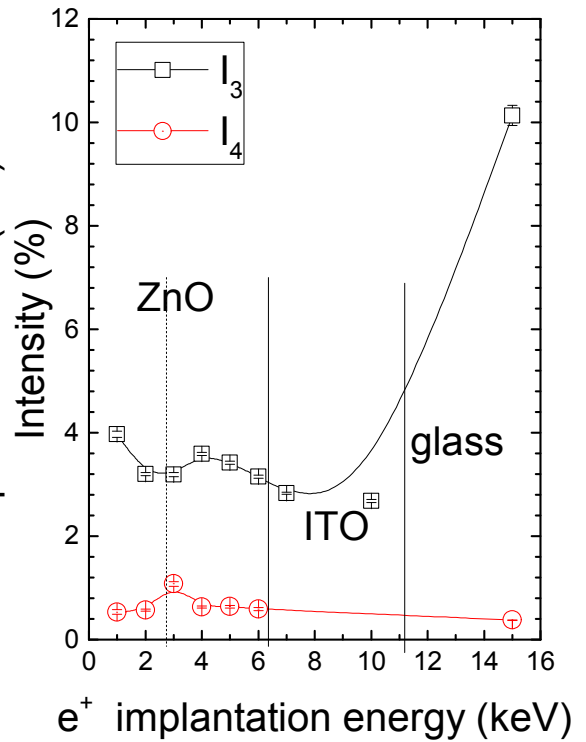
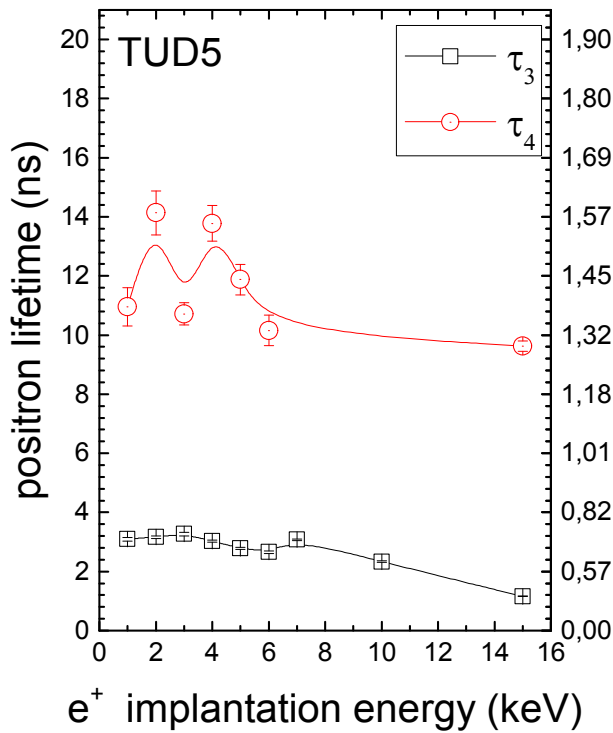
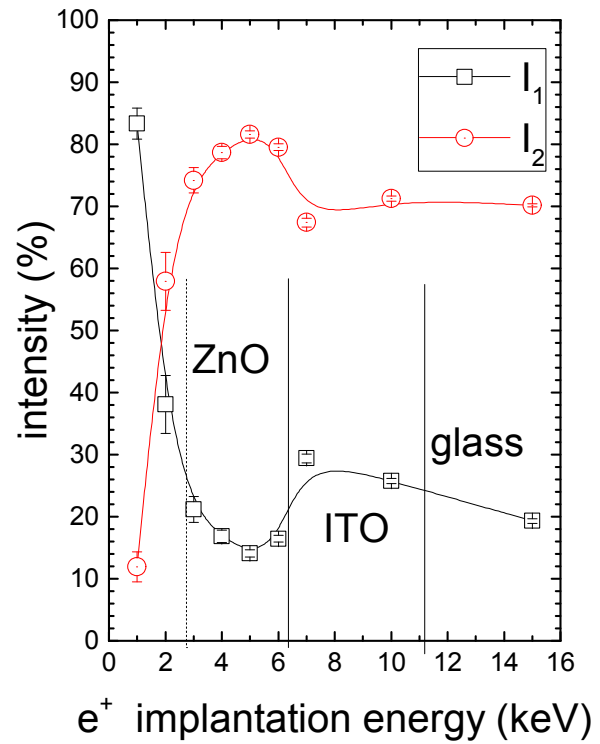
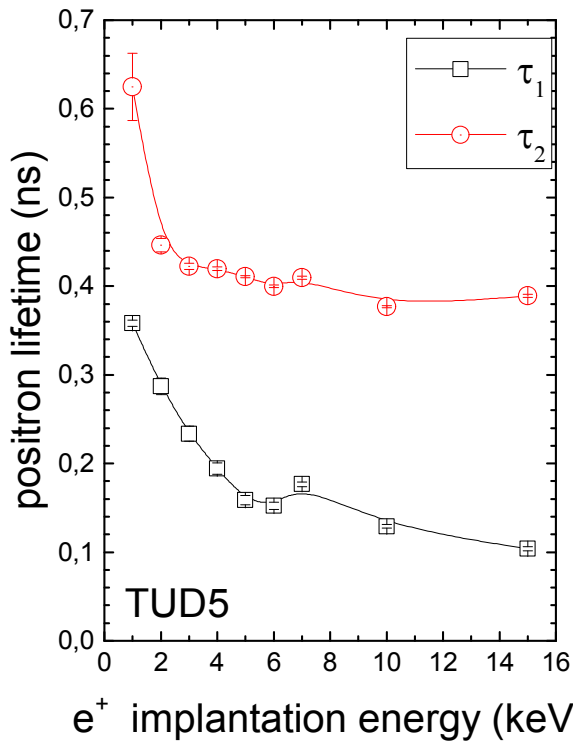


Fig S12: Depth profile derived from the curve fitting of the PALS spectra of ZnO film on ITO/glass substrate (*sample 3*) depicting values of the lifetime component τ_1 - τ_4 in dependence of positron implantation energy. (a) Lifetime components τ_1 and τ_2 . (b) Lifetime components τ_3 and τ_4 as well pore diameters calculated therefrom.

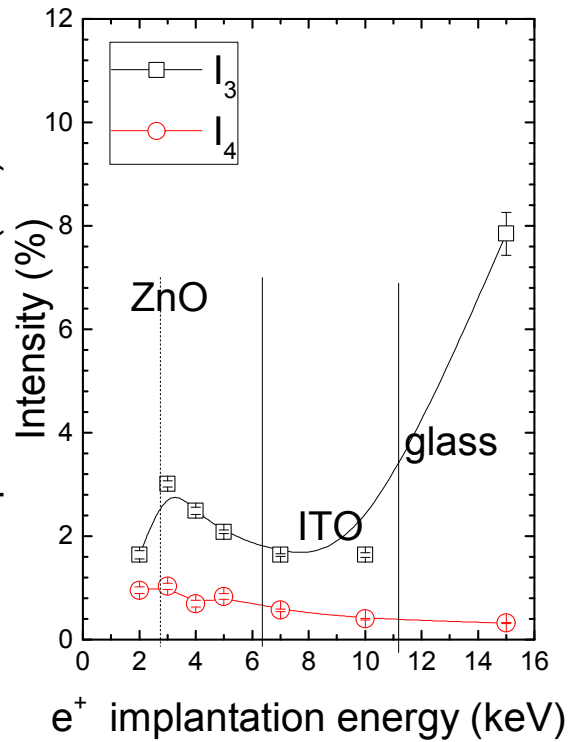
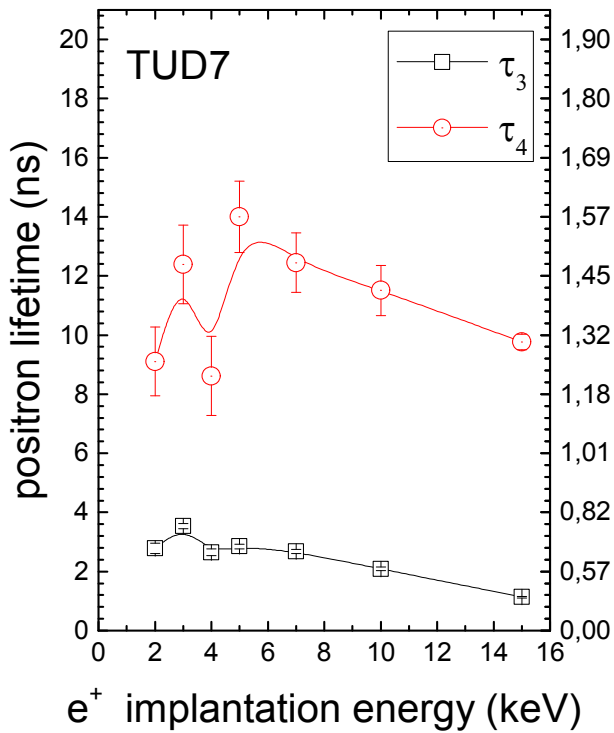
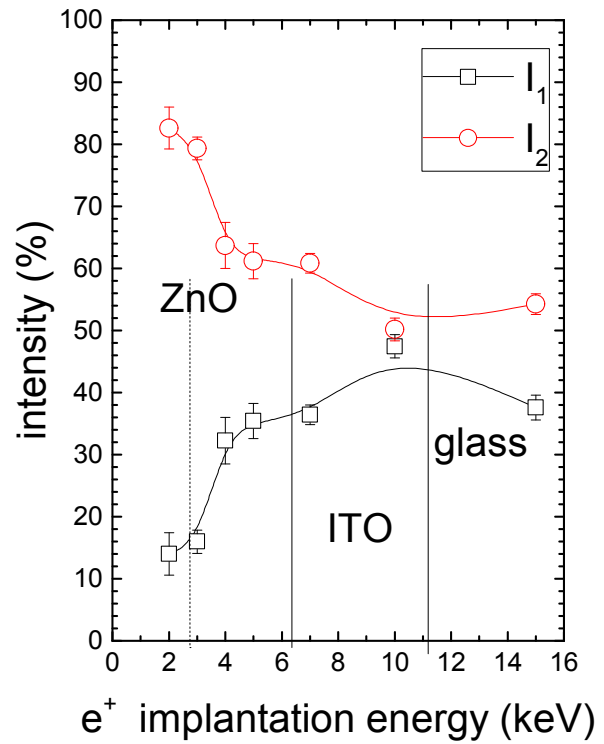
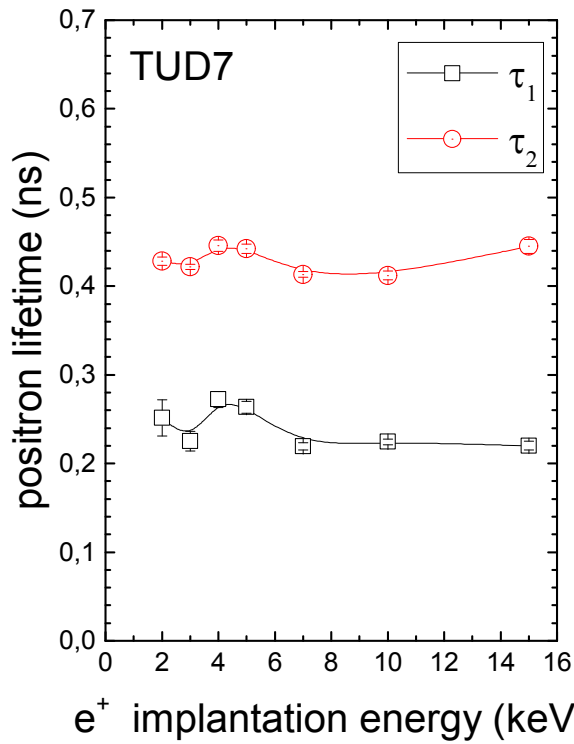


Fig S13: Depth profile derived from the curve fitting of the PALS spectra of ZnO film on ITO/glass substrate (*sample 4*) depicting values of the lifetime component τ_1 - τ_4 in dependence of positron implantation energy. (a) Lifetime components τ_1 and τ_2 . (b) Lifetime components τ_3 and τ_4 as well pore diameters calculated therefrom.

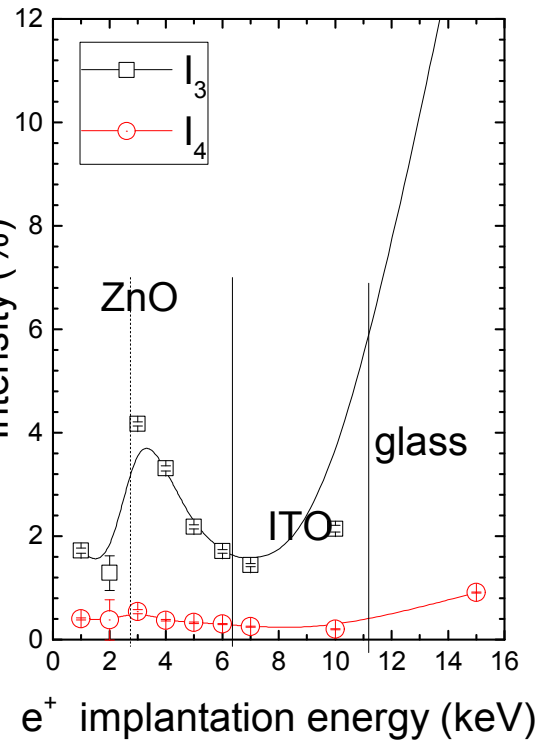
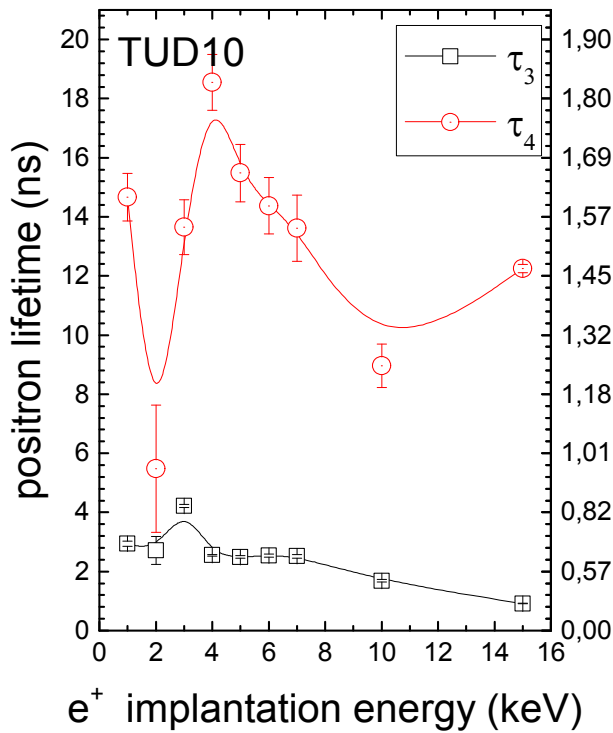
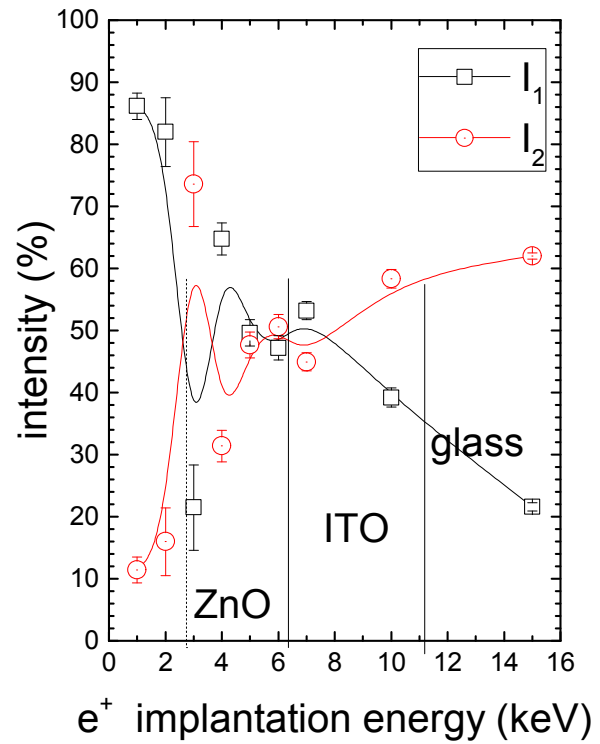
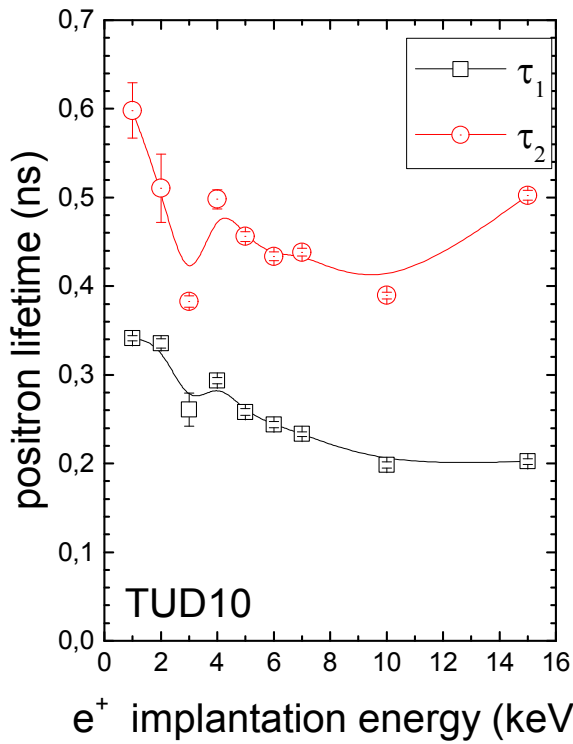


Fig S14: Depth profile derived from the curve fitting of the PALS spectra of ZnO film on ITO/glass substrate (*sample 5*) depicting values of the lifetime component τ_1 - τ_4 in dependence of positron implantation energy. (a) Lifetime components τ_1 and τ_2 . (b) Lifetime components τ_3 and τ_4 as well pore diameters calculated therefrom.

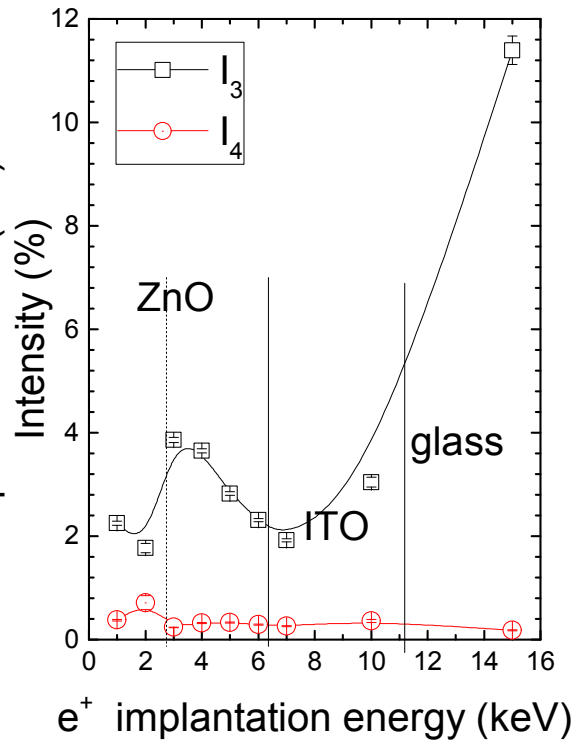
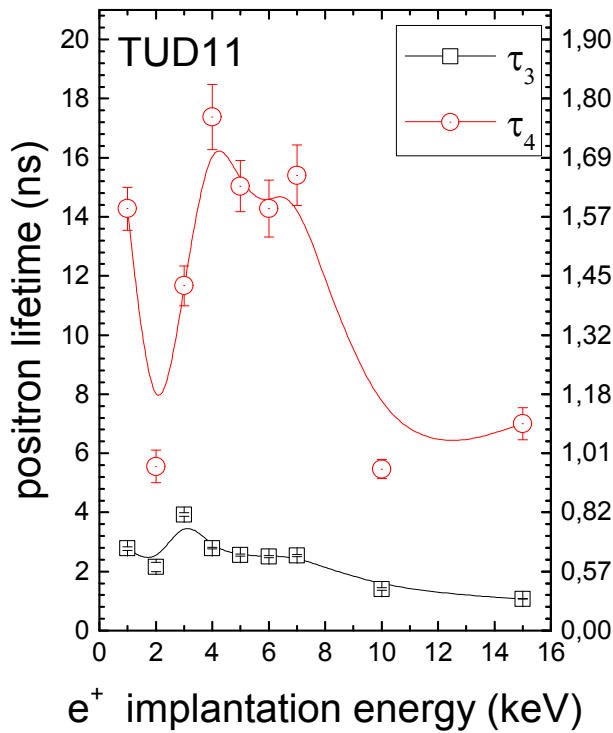
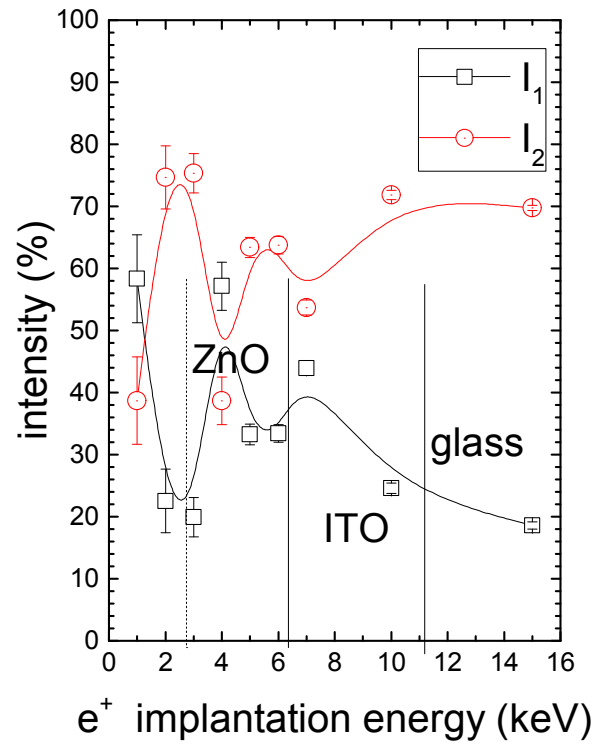
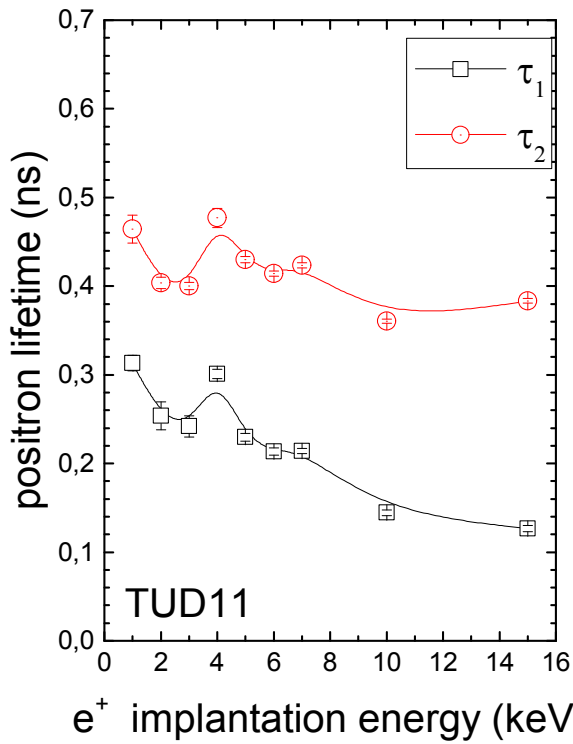


Fig S15: Depth profile derived from the curve fitting of the PALS spectra of ZnO film on ITO/glass substrate (*sample 6*) depicting values of the lifetime component τ_1 - τ_4 in dependence of positron implantation energy. (a) Lifetime components τ_1 and τ_2 . (b) Lifetime components τ_3 and τ_4 as well pore diameters calculated therefrom.

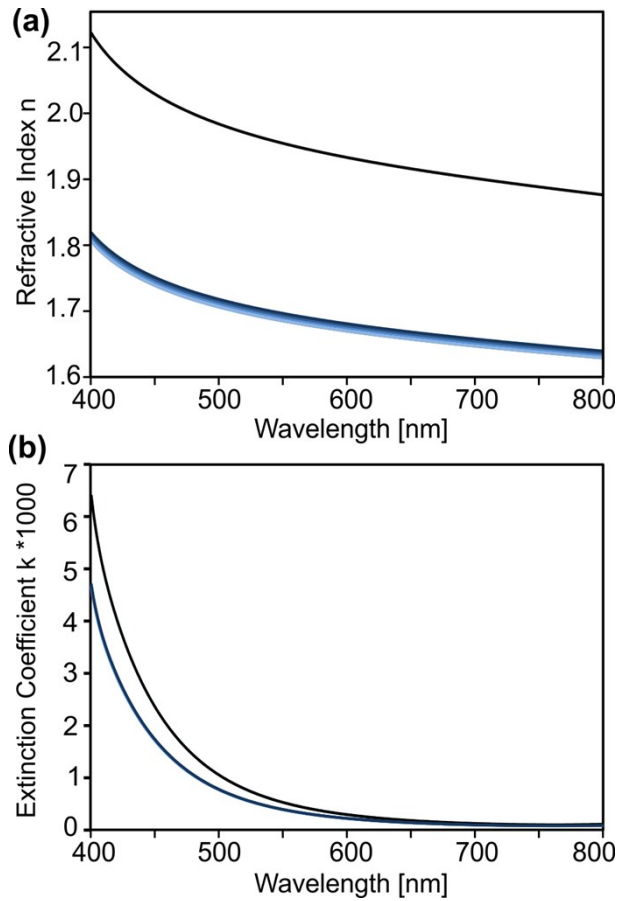


Fig S16: Optical constants of a ZnO layer in a ZnO/ITO/glass stack (samples #1-#4, blue lines) resulting from the curve fitting procedure as well for a ZnO single crystal (reference from software package, black line).

#	d [nm]	EMA [%]	MSE
1	23.02	-	5.698
2	64.71	26.2	8.985
3	110.91	27.3	5.433
4	178.45	24.6	17.033
5	104.71	24.9	8.731
6	155.00	20.0	27.41

Table S1: Results of curve fitting procedure (EMA effective medium approximation, MSE mean square error) for determination of the thickness d of the ZnO layers on ITO/glass substrates at 15/30 V for 30 to 120 min (#1-#4) as well as samples annealed at 250°C (#5 and #6).